Acta Pharmaceutica Sinica B 2020;10(6):1061−1072

Chinese Pharmaceutical Association
Institute of Materia Medica, Chinese Academy of Medical Sciences

Acta Pharmaceutica Sinica B

www.elsevier.com/locate/apsb
www.sciencedirect.com

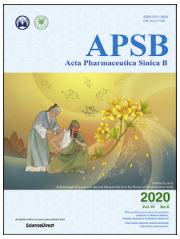

ORIGINAL ARTICLE

Arsenic trioxide induces regulatory functions of plasmacytoid dendritic cells through interferon-α inhibition

Yishan Ye[a,b], Laure Ricard[a], Lama Siblany[a], Nicolas Stocker[a], Frédéric De Vassoigne[c], Eolia Brissot[a,c], Baptiste Lamarthée[a], Arsène Mekinian[a,d], Mohamad Mohty[a,c], Béatrice Gaugler[a], Florent Malard[a,c,*]

[a]*Sorbonne Université, INSERM, Centre de Recherche Saint-Antoine (CRSA), Paris F-75012, France*
[b]*Bone Marrow Transplantation Center, the First Affiliated Hospital, School of Medicine, Zhejiang University, Hangzhou 310003, China*
[c]*AP-HP, Hôpital Saint-Antoine, Service d'Hématologie Clinique et Thérapie Cellulaire, Paris F-75012, France*
[d]*AP-HP, Hôpital Saint-Antoine, Service de Médecine Interne et de l'Inflammation-(DHU i2B), Paris F-75012, France*

Received 7 July 2019; received in revised form 4 December 2019; accepted 16 December 2019

KEY WORDS

Arsenic trioxide;
Plasmacytoid dendritic cell;
Immunotherapy;
Systemic sclerosis;
IFN-I

Abstract Arsenic trioxide (As_2O_3) is recently found to have therapeutic potential in systemic sclerosis (SSc), a life-threatening multi-system fibrosing autoimmune disease with type I interferon (IFN-I) signature. Chronically activated plasmacytoid dendritic cells (pDCs) are responsible for IFN-I secretion and are closely related with fibrosis establishment in SSc. In this study, we showed that high concentrations of As_2O_3 induced apoptosis of pDCs *via* mitochondrial pathway with increased BAX/BCL-2 ratio, while independent of reactive oxygen species generation. Notably, at clinical relevant concentrations, As_2O_3 preferentially inhibited IFN-α secretion as compared to other cytokines such as TNF-α, probably due to potent down-regulation of the total protein and mRNA expression, as well as phosphorylation of the interferon regulatory factor 7 (IRF7). In addition, As_2O_3 induced a suppressive phenotype, and in combination with cytokine inhibition, it down-regulated pDCs' capacity to induce $CD4^+$ T cell proliferation, Th1/Th22 polarization, and B cell differentiation towards plasmablasts. Moreover, chronically activated pDCs from SSc patients were not resistant to the selective IFN-α inhibition, and regulatory phenotype induced by As_2O_3. Collectively, our data suggest that As_2O_3 could

*Corresponding author. Tel.: +33 149282629; fax : +33 149283375.
E-mail address: florent.malard@inserm.fr (Florent Malard).

Peer review under responsibility of Institute of Materia Medica,Chinese Academy of Medical Sciences and Chinese Pharmaceutical Association.

https://doi.org/10.1016/j.apsb.2020.01.016

target pDCs and exert its treatment efficacy in SSc, and more autoimmune disorders with IFN-I signature.

1. Introduction

Arsenic trioxide (As_2O_3), an old drug well-known for its rediscovery in the treatment of acute promyelocytic leukemia (APL)[1], was shown to have therapeutic potential in a number of mouse models of autoimmune disorders including systemic sclerosis (SSc)[2,3], with largely unknown mechanism. Apoptosis induction and NF-κB pathway inhibition are two mechanisms generally known for As_2O_3 efficacy, but are not disease-specific[4,5].

Plasmacytoid dendritic cells (pDCs) are a unique subset of dendritic cells specialized in secreting high levels of type-I interferons (IFN-I), and are lately identified to play crucial pathogenetic role in SSc[6]. Thus, in a SSc mouse model with bleomycin-induced fibrosis, depletion of pDCs not only prevented the disease initiation, but ameliorated the established fibrosis[7,8]. Furthermore, in human, abnormally activated pDCs are infiltrated in the target organs such as skin, lung and bronchoalveolar lavage, and secrete IFN-α and CXCL4, which are both hallmarks of SSc[8,9].

Abnormal T and B cell responses are both key factors in the pathogenesis of SSc[10−12]. Upon activation by different signals, pDCs mature and present antigen to $CD4^+$ T cells, leading to Th1, Th2, Th17 or Treg responses[13−15]. On the other hand, IFN-α and IL-6 secreted by pDCs, as well as cell-to-cell contacts mediate the differentiation of B cells into plasmablasts and immunoglobulin-secreting plasma cells[16−18]. Overall, pDCs appear to be a promising therapeutic target in SSc treatment.

We conducted experiments to look into how As_2O_3 affects pDCs from both healthy donors and SSc patients, and to investigate the underlying mechanisms.

2. Materials and methods

2.1. Media and reagents

Complete medium was RPMI-1640 supplemented with 1 mmol/L sodium pyruvate, 2 mmol/L L-glutamine, MEM vitamin solutions, 100 U/mL penicillin, 100 μg/mL streptomycin and 10% heat-inactivated fetal bovine serum (all from Thermo Fisher Scientific, Villebon-sur-Yvette, France). CpG oligodeoxyribonucleotides (ODNs) are toll-like receptor 9 (TLR9) agonists. 1.5 μmol/L of class A CpG ODN 2216 (CpG-A), 1.5 μmol/L of class B CpG ODN 2006 (CpG-B), or 1 μmol/L of class P CpG ODN 21798 (CpG-P) (all from Miltenyi Biotec, Paris, France) were used to activate pDCs *in vitro* in this study. CpG-A is a strong inducer of type I IFNs, whereas CpG-B is a potent stimulator of maturation and the production of cytokines and chemokines. CpG-P exhibits properties of both CpG-A and CpG-B. The stock solution of As_2O_3 (6672 μmol/L) was reconstituted by dissolving As_2O_3 (Sigma−Aldrich, Saint-Quentin Fallavier, France) powder into distilled water and stored in 4 °C fridge. The solution was then diluted in complete medium to reach the target concentrations. For control condition a similar volume of complete medium was added.

2.2. pDC isolation and culture

Peripheral blood mononuclear cells (PBMCs) were obtained from buffy coats by Ficoll density centrifugation, from healthy donors (Etablissement Français du Sang, Paris Saint-Antoine-Crozatier, France) or untreated SSc patients (Hôpital Saint-Antoine, Paris, France) after informed consent. The study was approved by the local institutional review board and the Comité de Protection des Personnes Ile-de France VII (CPP Ouest-1, reference 2017-A03380-53). pDCs were negatively selected with EasySep™ Human Plasmacytoid DC Enrichment Kit (Stem cell, Grenoble, France). The purity of isolated pDCs, verified by flow cytometry using PE-Vio770-BDCA2 (Miltenyi Biotec), ECD-CD123 (Beckman Coulter, Villepinte, France), was >90%.

2.3. pDC viability and apoptosis

Isolated pDCs were cultured in the presence of 10 ng/mL IL-3 (Miltenyi Biotec), or activated with CpG-A/CpG-P in the presence of the indicated doses of As_2O_3. Viability and apoptosis were checked with Fixable Viability Dye eFluor™ 506 (FVD, Thermo Fisher Scientific) and FITC Annexin V (Biolegend, Ozyme, Saint-Quentin-Fallavier, France). FVD^-Annexin V^- cells were regarded as viable, FVD^+ cells as dead, and FVD^-Annexin V^+ cells as apoptotic. For NAC (Sigma−Aldrich) treatment, pDCs were pre-treated with 1 mmol/L of NAC for 1 h, washed and placed in culture for 6 h. For BCL-2 and BAX staining, isolated pDCs were cultured for 6 h in complete culture medium in the presence of 10 ng/mL IL-3, or activated with CpG-A in the presence of 5 μmol/L As_2O_3. Afterwards cells were stained with PE-BCL-2 (BD Biosciences, Le Pont de Claix, France) and Alexa Fluor® 488-BAX (Biolegend, Ozyme) or the corresponding isotype controls, using the FOXP3/Transcription Factor Staining Buffer Set (Thermo Fisher Scientific).

2.4. Reactive oxygen species

Isolated pDCs were cultured for 30 min in complete medium in the presence of 10 ng/mL IL-3, with or without activation with CpG-A and 5 μmol/L As_2O_3. Instead of As_2O_3, pDCs were cultured simultaneously with 200 μmol/L of *tert*-butyl hydroperoxide as positive control. For negative control, pDCs were pre-treated with 1 mmol/L of antioxidant *N*-acetylcysteine (NAC) for 1 h. Reactive oxygen species (ROS) level was detected with CellROX® Green Flow Cytometry Assay Kits (Thermo Fisher Scientific).

2.5. Cytokine secretion analysis

PBMCs were incubated with increasing doses of As_2O_3, activated with CpG-A for 6 h, and 1 μL/mL Golgi plug (BD Biosciences) was added in the last 3 h. The cells were firstly stained with FVD eFluor™ 506, then with PE-Vio770-BDCA2 (Miltenyi Biotec)

and ECD-CD123 (Beckman Coulter). Cells were then stained with FITC-IFN-α and APC-Vio770-TNF-α (both from Miltenyi Biotec) with Cytofix/Cytoperm Buffer (BD Biosciences).

2.6. Cell signaling staining

Isolated pDCs were cultured overnight in the absence of IL-3, with or without CpG-A and 1 μmol/L of As_2O_3. Afterwards, the cells were fixed with Cytofix™ Fixation Buffer (BD Biosciences), permeabilized with Phosflow™ Perm Buffer III (BD Biosciences), and then stained with APC-interferon regulatory factor 7 (IRF7) and PE-IRF7 pS477/pS479 (both from Miltenyi Biotec).

2.7. Gene expression analysis

Isolated pDCs were cultured for 6 h in the absence of IL-3, with or without CpG-A and 1 μmol/L of As_2O_3. RNA was then extracted using RNAeasy Mini kit (QIAGEN, Les Ulis, France). RNA was subjected to reverse transcription (High Capacity RNA-to-cDNA Master Mix, Thermo Fisher Scientific) and quantified by real-time quantitative PCR using commercially available primer/probes sets (Assay-On-Demand, Thermo Fisher Scientific): *GAPDH* (Hs99999905_m1) and *IRF7* (Hs01014809_g1). Real-time PCR was performed on a 7500 Fast Dx Real-Time PCR Instrument (Thermo Fisher Scientific). Relative expressions for the mRNA transcripts were calculated using the $\Delta\Delta C_t$ method and *GAPDH* mRNA transcript as reference.

2.8. Phenotype evaluation

After 24 h of culture, pDCs were harvested and stained with FVD eFluor™ 506, treated with human Fc block (Miltenyi Biotec) and stained with the following antibodies: AA750-CD80, PC5.5-CD86, FITC-HLA-DR (Beckman Coulter), PE-CCR7 (Thermo Fisher Scientific), APC-programmed cell death-ligand 1 (PD-L1, BD Biosciences) or the corresponding isotype controls. The relative fluorescence intensity (RFI) ratios were calculated by normalizing the RFI of the indicated to the condition of non-activated pDCs without As_2O_3 treatment.

2.9. Mixed lymphocyte reaction (MLR)

For the pDC/$CD4^+$ T cell coculture system, pDCs were cultured for 24 h with 0.25−0.5 μmol/L As_2O_3 in the presence of 10 ng/mL IL-3, simultaneously activated with CpG-A or CpG-B, and washed twice before co-culture. Allogeneic naïve $CD4^+$ T cells were isolated from PBMC using MagniSort™ Human CD4 Naïve T cell Enrichment Kit (Thermo Fisher Scientific). After isolation, $CD4^+$ T cells were labeled with Cell Proliferation Dye eFluor® 450 (Thermo Fisher Scientific) and co-cultured with pDCs at a 2:1 ratio for 7 days. T cell proliferation was assessed at day-5 of culture by flow cytometry. For intracellular cytokine detection, cells were harvested at day-7 of culture and stimulated for 5 h with 25 ng/mL phorbol-12-myristate-13-acetate (PMA, Sigma−Aldrich) and 1 μg/mL ionomycin (Sigma−Aldrich), and 1 μL/mL Golgi plug. Afterwards, cells were stained with FVD 575 V (BD Biosciences), followed by staining with PE/Dazzle 594-CD3 (Biolegend) and PC7-CD4 (BD Biosciences). Finally, cells were stained with PE-IFN-γ, APC-Vio770-TNF-α, eFluor660-IL-22 (Thermo Fisher Scientific) and Vio-515-IL-10 (Miltenyi) with Cytofix/Cytoperm Buffer (BD Biosciences).

For the pDC/B cell co-culture system, pDCs were pre-treated for 24 h with 0.5 μmol/L As_2O_3 in the presence of 10 ng/mL IL-3, and washed twice before co-culture. Syngeneic $CD19^+$ B cells were isolated from PBMC using MagniSort® Human CD19 Positive Selection Kit (Thermo Fisher Scientific), and co-cultured with pDCs at a 3:1 ratio, in the presence of 1 μmol/L CpG-P for 3 days. Cells were then stained with FITC-CD19, ECD-CD24, PC5.5-CD38 (all from Beckman Coulter), and BV421-CD27 (Biolegend).

2.10. ELISA

ELISA kits of IFN-α (Thermo Fisher Scientific), TNF-α, IL-6 (PeproTech, Neuilly-sur-Seine, France) and CXCL10 (Biolegend) were used to detect these cytokine/chemokine concentrations in supernatants of pDC cultures.

2.11. Flow cytometry

Analyses were performed with CytoFLEX Flow Cytometer (Beckman Coulter) and Kaluza Flow Cytometry Analysis Software version 1.5a (Beckman Coulter).

2.12. Statistical analysis

The Student's *t*-test was used for comparison between conditions. All data were analyzed using GraphPad Prism 5.0 (GraphPad Software, San Diego, CA, USA). A $P < 0.05$ was considered to be significant.

3. Results

3.1. High concentrations of As_2O_3 induces pDC apoptosis via mitochondrial pathway with BAX/BCL-2 ratio increase

In the treatment of APL, patients' plasma As_2O_3 reaches the peak level of around 6 μmol/L about 3−4 h after administration and quickly decreases to a stable concentration between 0.5 and 3 μmol/L[19]. Therefore, concentrations up to 2 μmol/L were considered as clinical relevant. We cultured pDCs purified from healthy donors in the presence of different doses of As_2O_3 for 6 or 24 h, respectively. After 6 h of treatment, up to 2 μmol/L of As_2O_3 induced neither significant increase of pDC apoptosis (Fig. 1A and B) nor decrease of viable pDCs (Fig. 1A and C). Five μmol/L of As_2O_3, however, significantly increased pDC apoptosis (Fig. 1A and B) and decreased the pDC viability (Fig. 1A and C). Meanwhile, there was a significantly lower degree of apoptosis in the CpG-A activated group as compared with the non-activated group, revealing a protective nature of CpG-A activation against apoptosis induction (Fig. 1B). After 24 h, there was an As_2O_3 dose-dependent decrease of viable pDC percentages, with concentrations equal or over 1 μmol/L significantly decreased viability of both non-activated and CpG-A activated pDCs. The CpG-P activated pDCs were more resistant to As_2O_3, whose viability significantly decreased with equal or over 2 μmol/L (Fig. 1D). Moreover, for all the concentrations investigated, percentages of apoptotic pDCs were below 5% after 24 h culture, probably due to the death of apoptotic cells between 6 and 24 h (data not shown). Accordingly, we used higher concentration (5 μmol/L) of As_2O_3 for pDC apoptotic tests, and non-toxic

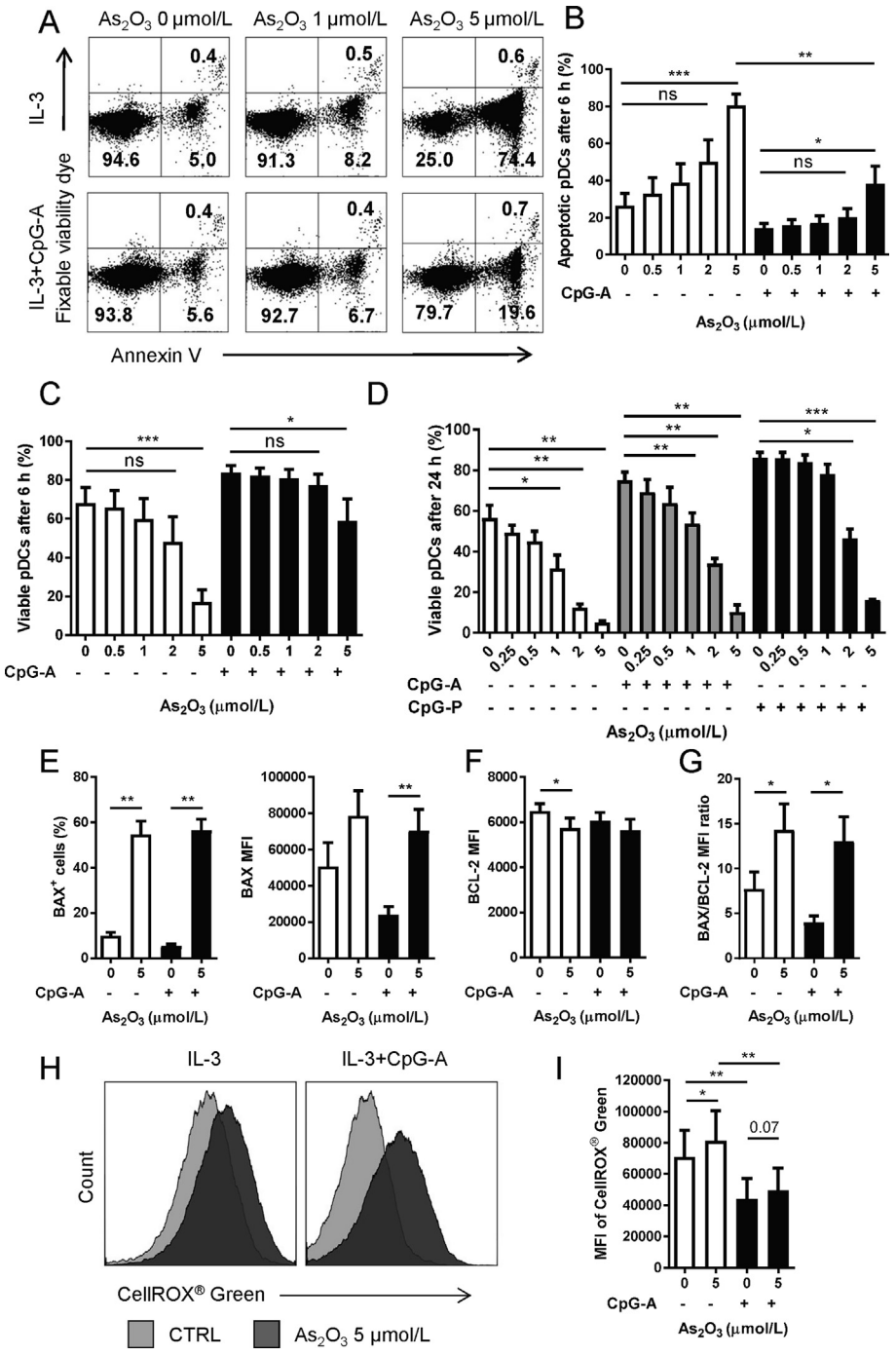

Figure 1 As_2O_3 induces pDC apoptosis *via* mitochondrial pathway with BAX/BCL-2 ratio increase. Purified pDCs were cultured with indicated doses of As_2O_3 before tests. (A) Representative graph of pDC apoptosis after 6 h of culture [$n = 4$ independent healthy donors (HD)]. Percent of (B) apoptotic or (C) viable cells after 6 h culture with 0−5 μmol/L As_2O_3 ($n = 4$ HD). (D) Percent of viable cells after 24 h culture ($n = 4$ HD) (E) Percent of BAX^+ cells ($n = 4$ HD), MFI of BAX ($n = 4$ HD), (F) MFI of BCL-2 ($n = 4$ HD), and (G) BAX/BCL-2 MFI ratio ($n = 4$ HD) after 6 h culture with 5 μmol/L As_2O_3. (H) Representative graph of intracellular ROS with (black) or without (grey) 5 μmol/L As_2O_3 for 30 min ($n = 5$ HD). (I) MFI of the ROS ($n = 5$ HD). Data are represented as mean ± SEM. $^*P < 0.05$, $^{**}P < 0.01$ and $^{***}P < 0.001$ by *t*-test.

concentrations of As_2O_3 for all the following functional tests on pDCs.

BAX and BCL-2 are key members of the BCL-2 family proteins within the mitochondrial apoptotic pathway, and the BAX to BCL-2 ratio determines cell survival/death following an apoptotic stimulus[20]. We observed that BAX was greatly upregulated, while BCL-2 was slightly decreased in pDCs treated with 5 μmol/L of As_2O_3 for 6 h (Fig. 1E and F and Supporting Information Fig. S1), leading to a significantly increased BAX/BCL-2 ratio (Fig. 1G). As_2O_3 is a well-known inducer of oxidative stress, an initiator of

apoptosis. However, we observed that although 5 μmol/L of As_2O_3 increased the intracellular ROS in non-activated pDCs (Fig. 1H and I), the anti-oxidant NAC pre-treatment, which significantly reduced the intracellular ROS level (Supporting Information Figs. S2A and B) without affecting pDCs viability (Figs. S2C and D), did not prevent the As_2O_3-induced pDC apoptosis (Fig. S2E).

3.2. *Clinical-relevant As_2O_3 inhibits cytokine secretion of pDCs, with special potency on IFN-α*

PBMCs were incubated with CpG-A and up to 2 μmol/L As_2O_3 for 6 h, which induced neither pDC death nor apoptosis, and IFN-α/TNF-α secretions were analyzed by intracellular staining on gated viable pDCs (Supporting Information Figs. S3A and B). Surprisingly, we observed that As_2O_3 significantly inhibited the production of IFN-α dose-dependently, but not TNF-α, for either percentages of cytokine secretion cells (Fig. 2A) or the mean florescent intensity (MFI) of cytokine expressions of all gated viable pDCs (Supporting Information Figs. S4A and B). However, ELISA analysis of supernatants of purified pDCs after 24 h culture showed that non-lethal As_2O_3 inhibited secretion of both IFN-α and TNF-α significantly (Fig. 2B). Moreover, IL-6 and CXCL10 productions were also slightly decreased but not statistically significant (Supporting Information Fig. S5).

3.3. *As_2O_3 blocks IFN-α secretion from pDCs via IRF7 inhibition*

Decrease of TNF-α, IL-6 and CXCL10 secretion from pDCs were probably due to As_2O_3 inhibition of the NF-κB pathway[4,21]. However, the reason for the quick and potent inhibition of IFN-α remained to be elucidated. We focused on IRF7, a crucial and specific regulator of both the induction and maintenance of IFN-α secretion by pDCs[22]. Overnight incubation with 1 μmol/L of As_2O_3 induced a significant decrease of both the percentage of $IRF7^+$ pDCs and MFI of IRF7 from both non-activated and CpG-A activated pDCs, gated on viable pDCs (Fig. 2C–E). Meanwhile, the percentage of phospho-$IRF7^+$ pDCs was also significantly decreased in both non-activated and CpG-A activated conditions (Fig. 2F and G). Further RT-PCR experiments demonstrated the inhibition on the mRNA level, in both non-activated and CpG-A activated conditions (Fig. 2H).

3.4. *As_2O_3 induces regulatory phenotype of pDCs*

It has been shown that As_2O_3 induced a suppressive phenotype on immature DCs[23]. We addressed whether pDC maturation could also be influenced by As_2O_3 treatment. For this purpose, isolated pDCs were incubated with non-lethal doses of As_2O_3 for 24 h, simultaneously activated with CpG-A, and checked for the expression of maturation markers (Fig. 3A). The results showed that 0.5 μmol/L of As_2O_3 significantly decreased the RFI ratio of CD80, CD86, and HLA-DR, as well as the percentages of $CD86^+$ and $CCR7^+$ activated pDCs. We also observed an up-regulated expression of PD-L1 (Fig. 3B and C).

3.5. *As_2O_3 impairs pDCs' capacity to induce $CD4^+$ T cell proliferation and Th1/Th22 polarization*

We used a pDC/$CD4^+$ T cell co-culture system to investigate As_2O_3' effects on pDCs' capacity to induce T cell proliferation and polarization. Flow cytometry analysis showed that when pDCs were pretreated with 0.5 μmol/L of As_2O_3 for 24 h, together with CpG-B activation, they induced significantly lower percentages of proliferating $CD4^+$ T cells after 5 days of co-culture (Fig. 4A and B). We then investigated the effect of As_2O_3 treatment on the pDC capacity to polarize allogeneic naïve $CD4^+$ T cells. Flow cytometry analysis showed that when naïve $CD4^+$ T were co-cultured with activated pDCs pre-treated with As_2O_3, there was a significant decrease in the percentages of IFN-γ (Fig. 4C and D) and IL-22 (Fig. 4E and F) positive proliferating $CD4^+$ T cells after 7 days. However, As_2O_3 did not alter the percentages of IL-10 or TNF-α positive proliferating $CD4^+$ T cells significantly (Supporting Information Fig. S6).

3.6. *As_2O_3 inhibits plasmablast differentiation of B cells*

We used a pDC/B cell co-culture model to investigate As_2O_3' effects on pDCs' capacity to induce B cell differentiation towards plasmablasts[24]. The flow cytometry results showed that pDCs, together with CpG-P, induced $CD27^{hi}CD38^{hi}$ plasmablast differentiation of syngeneic B cells. When pDCs were pretreated with 0.5 μmol/L of As_2O_3 for 24 h, significantly lower percentages of plasmablasts were induced (Fig. 5A and B). Given that IFN-α/IL-6 secretion and cell-to-cell contacts mediate pDC-induced B cell differentiation, we subsequently observed that 24 h culture of as low as 0.25 μmol/L of As_2O_3 decreased greatly the IFN-α secretion from CpG-P activated pDCs, with IL-6 inhibition shown at a higher concentration (Fig. 5C). Meanwhile, As_2O_3 significantly decreased $CD86^+$ pDCs, and increased PD-L1 expression on CpG-P activated pDCs (Fig. 5D), with the CD80, HLA-DR, and CCR7 expressions not significantly altered (Supporting Information Fig. S7).

3.7. *SSc pDCs are sensitive to As_2O_3-induced selective IFN-α inhibition, and regulatory phenotype*

In order to further investigate As_2O_3 as a potential therapeutic agent for SSc, we first tested As_2O_3 on PBMCs from 12 untreated SSc patients. After incubation with CpG-A and clinical relevant doses of As_2O_3 for 6 h, IFN-α production was inhibited dose-dependently, but not TNF-α from pDCs of SSc patients (Fig. 6A). We then checked how As_2O_3 affected the viability and phenotype of pDCs purified from 6 additional SSc patients (for all patients information, see Supporting Information Table S1). After 24 h of culture, 0.5 μmol/L of As_2O_3, which is non-lethal for pDCs from healthy donors, significantly decreased, albeit not hugely, the viability of both non-activated and CpG-A activated SSc pDCs (Fig. 6B). An increased BAX/BCL-2 ratio was also observed when these cells were cultured for 6 h with high dose of 5 μmol/L As_2O_3 (Fig. 6C–E). For phenotype, 24 h culture with 0.5 μmol/L of As_2O_3 decreased significantly both the MFI and the percentages of $CD80^+$ and $CD86^+$ SSc pDCs, while increased both the MFI and the percentage of PD-$L1^+$ SSc pDCs, with CCR7 and HLA-DR expressions unchanged (Fig. 6F and G).

4. Discussion

With this study, we concluded that in clinical conditions, As_2O_3 may induce pDC apoptosis during the first hours of drug administration. Afterwards, clinical relevant concentrations of As_2O_3 do not alter viability, but induce mostly functional

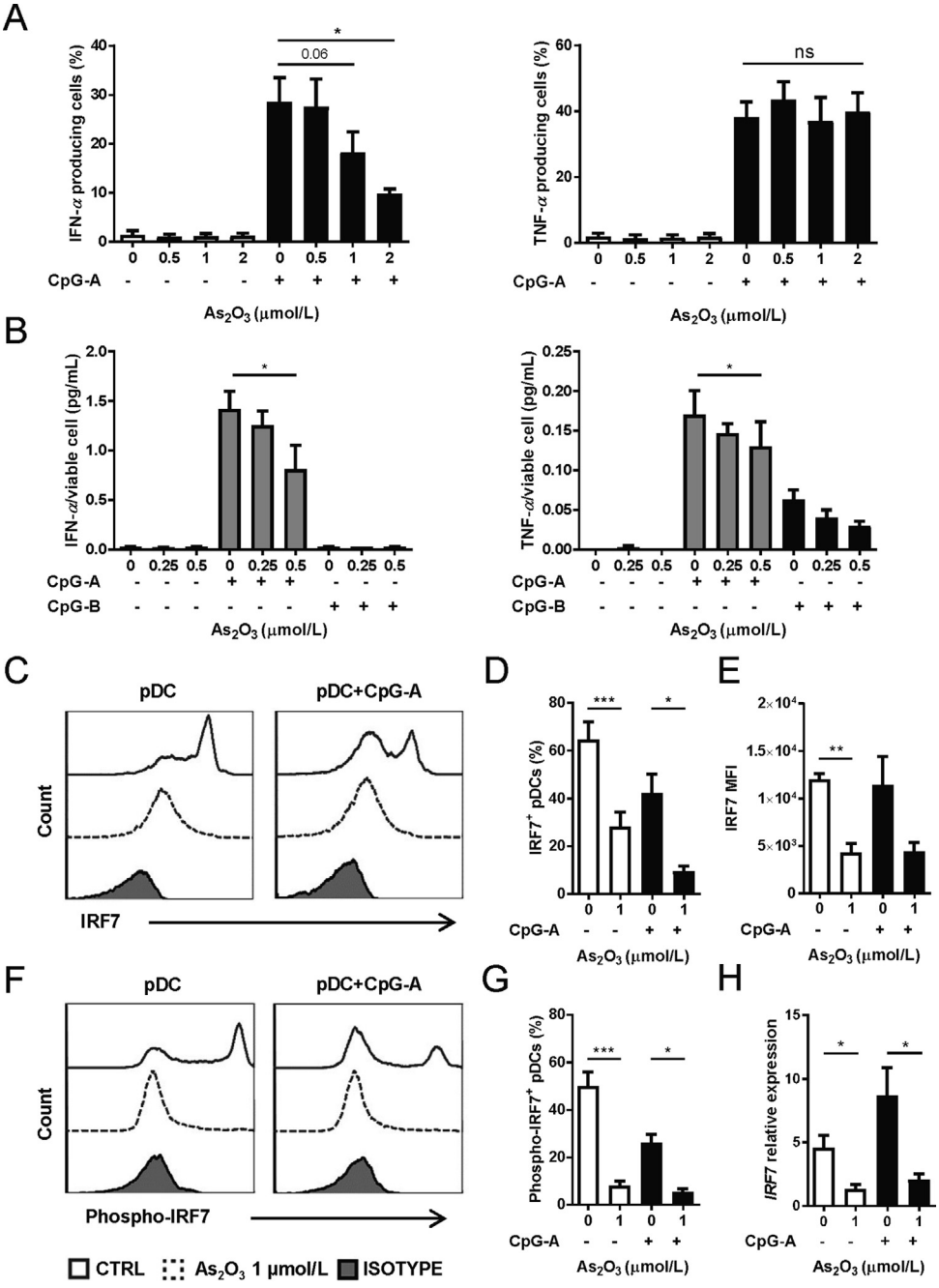

Figure 2 As_2O_3 preferentially blocks IFN-α production from pDCs *via* IRF7 inhibition. (A) Percent of IFN-α/TNF-α positive viable pDCs after PBMC incubation with indicated doses of As_2O_3 for 6 h ($n = 4$ HD). (B) Concentrations of indicated cytokines in supernatants of purified pDCs for 24 h with As_2O_3, normalized to concentration per viable cell ($n = 5$ HD). For (C) to (G), purified pDCs were cultured with 1 μmol/L As_2O_3 overnight before tests, gated on living cells. (C) and (F) Representative graph of IRF7 and phospho-IRF7, after incubation with (dotted line) or without As_2O_3 (solid line), and the isotype control (grey) ($n = 5$ HD). (D) Percent of $IRF7^+$ cells ($n = 5$ HD). (E) MFI of IRF7 ($n = 5$ HD). (G) Percent of $IRF7^+$ cells ($n = 5$ HD). (H) *IRF7* mRNA expression within purified pDCs cultured with 1 μmol/L As_2O_3 for 6 h ($n = 4$ HD). Data are represented as mean ± SEM. $^*P < 0.05$, $^{**}P < 0.01$ and $^{***}P < 0.001$ by *t*-test.

alterations of pDCs. The survival of the resting state pDCs depend predominantly on the mitochondrial BCL-2 pathway, while the survival of activated pDCs is regulated by several pathways[25,26]. The pro-apoptotic protein BAX and the anti-apoptotic protein BCL-2 are important players in the mitochondrial apoptotic pathway[27], and the BAX/BCL-2 ratio determines survival or death following an apoptotic stimulus[20]. We found that As_2O_3 induced a significantly increased BAX/BCL-2

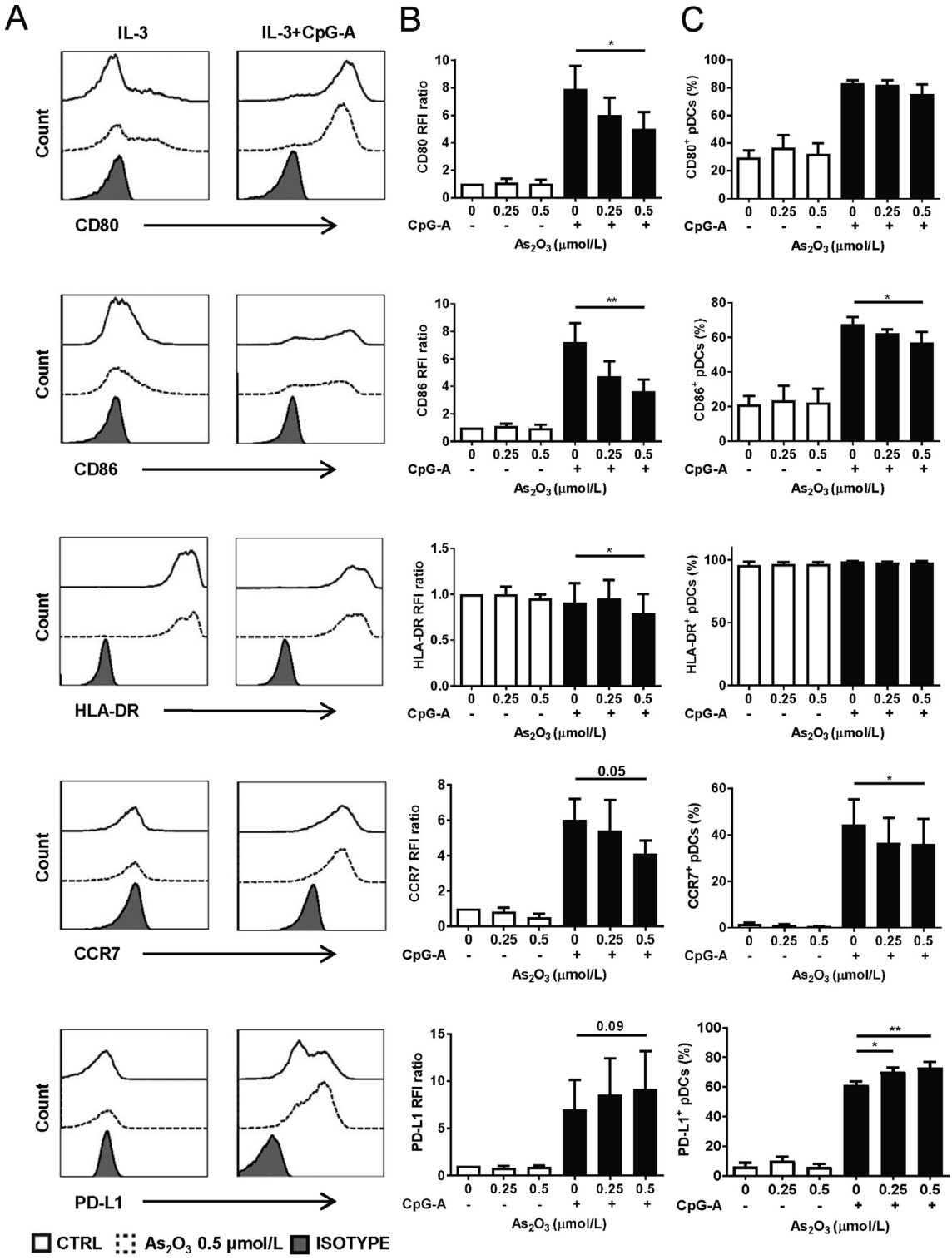

Figure 3 As_2O_3 induces regulatory phenotype of pDCs. Isolated pDCs were incubated with/without CpG-A activation, with indicated doses of As_2O_3 for 24 h before flow cytometry analysis. (A) Representative graph showing cells positive for the indicated surface molecule in the presence of 0.5 μmol/L As_2O_3 (dotted line), control (solid line) and the isotype control (grey) ($n = 4$ HD). (B) Relative fluorescence intensity (RFI) ratios of indicated surface molecules ($n = 4$ HD). (C) Percentages of positive cells for indicated surface molecule ($n = 4$ HD). Data are represented as mean ± SEM. $^{*}P < 0.05$, $^{**}P < 0.01$ by *t*-test.

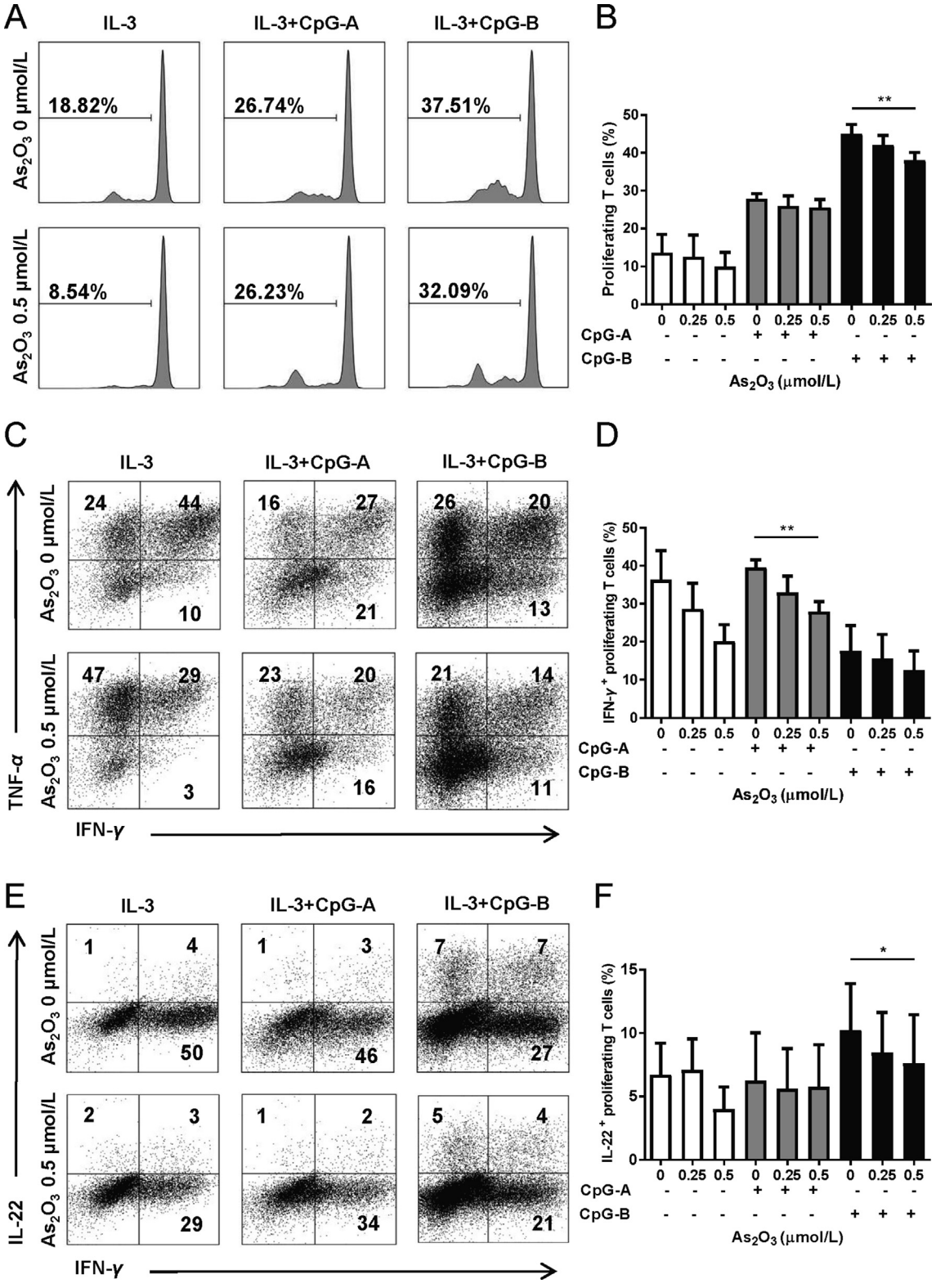

Figure 4 As_2O_3 impairs pDCs' capacity to induce $CD4^+$ T cell proliferation and Th1/Th22 polarization. A pDC/$CD4^+$ cell co-culture system was used. T cell proliferation and polarization was detected on day-5 and day-7 of co-culture, respectively. (A) Representative graph of cell proliferation ($n = 4$). (B) $CD4^+$ T cells negative for cell proliferation dye ($n = 4$). (C) Representative graph of IFN-γ^+ and TNF-α^+ proliferating T cells gated on cell proliferation dye-negative cells ($n = 4$). (D) Percent of IFN-γ^+ proliferating T cells ($n = 4$). (E) Representative graph of IFN-γ^+ and IL-22^+ proliferating T cells gated on cell proliferation dye-negative cells ($n = 4$). (F) % of IL-22^+ proliferating T cells ($n = 4$). Data are represented as mean ± SEM. $^*P < 0.05$, $^{**}P < 0.01$ by *t*-test.

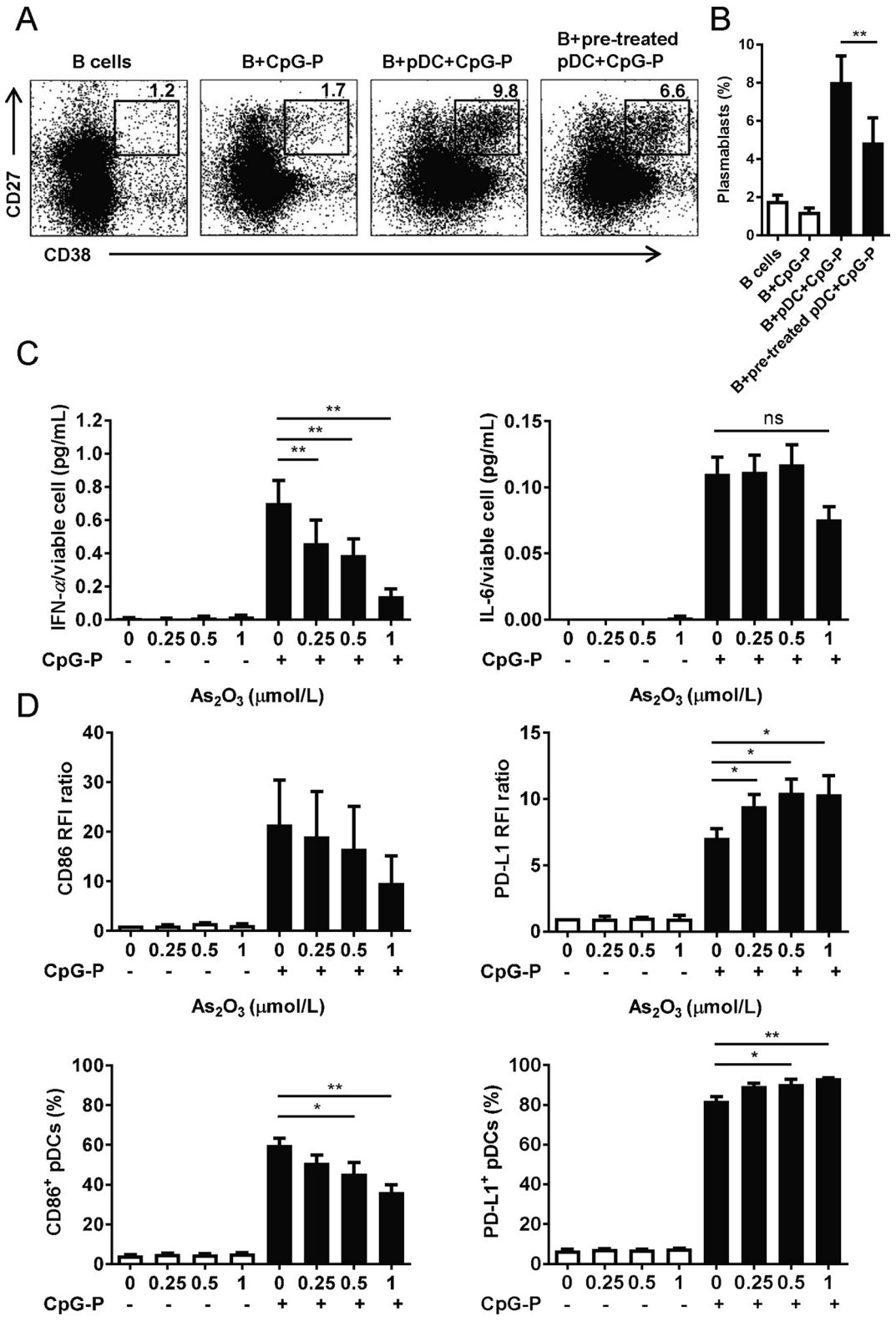

Figure 5 As_2O_3 reduces pDCs' ability to induce plasmablast differentiation of B cells. A pDC/B cell co-culture model was used. $CD38^{hi}CD27^{hi}$ plasmablast differentiation was analyzed on day-3 of co-culture. (A) Representative graph of $CD38^{hi}CD27^{hi}$ plasmablasts, gated on $CD19^{+}$ cells ($n = 4$). (B) Percent of $CD38^{hi}CD27^{hi}$ plasmablasts among all gated B cells ($n = 4$). For (C) to (D), isolated pDCs were incubated with/without CpG-P activation, with indicated doses of As_2O_3 for 24 h before analysis. (C) IFN-α and IL-6 concentrations in supernatants of purified pDCs ($n = 4$ HD). (D) RFI ratios and percentages of positive cells for CD86 and PD-L1 ($n = 4$ HD). Data are represented as mean ± SEM. $^{*}P < 0.05$, $^{**}P < 0.01$ by *t*-test.

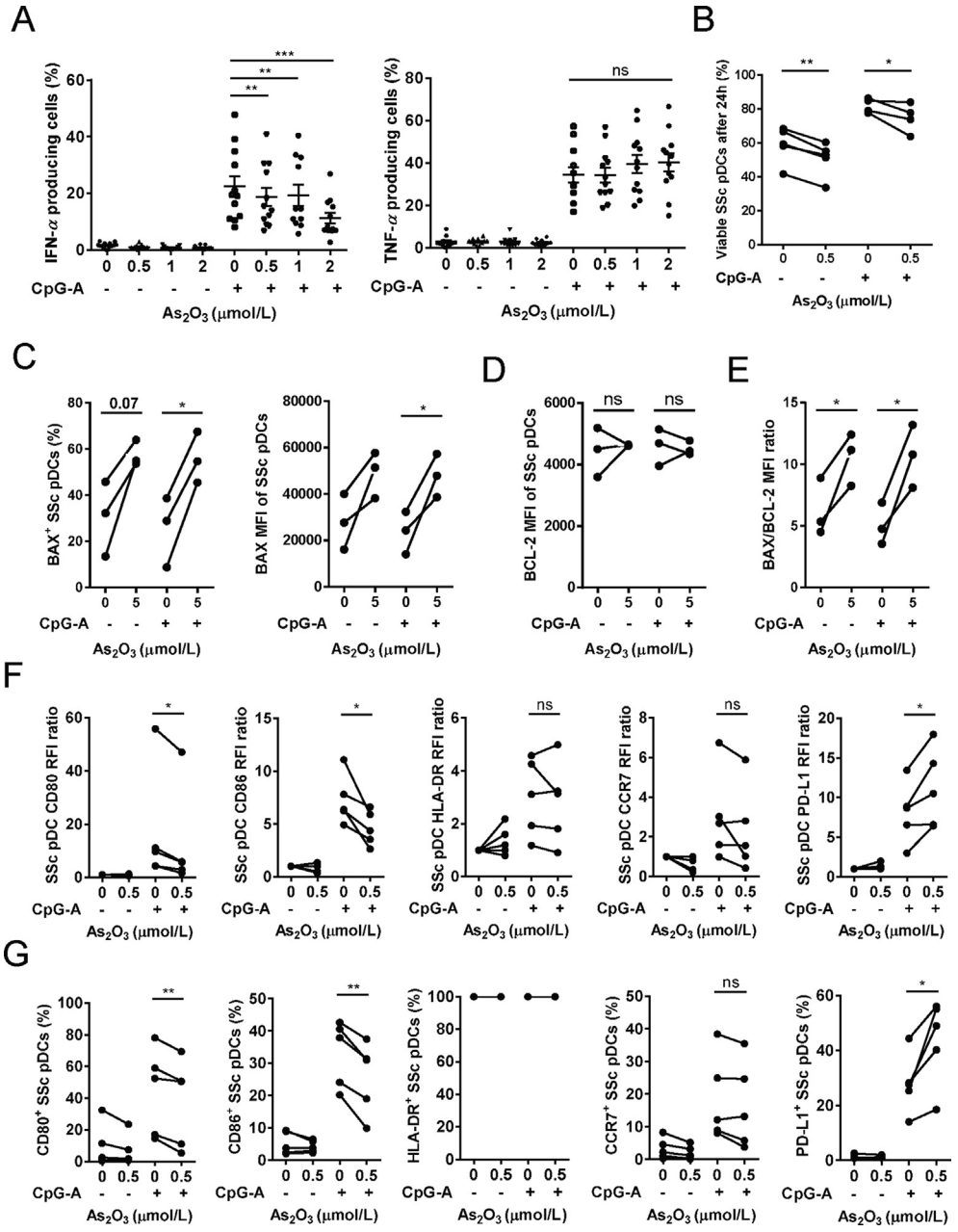

Figure 6 As_2O_3-induced pro-apoptotic effects, selective IFN-α inhibition, and regulatory phenotype are not resistant by SSc pDCs. (A) Percent of IFN-α and TNF-α positive pDCs after PBMCs from SSc patients were incubated with indicated doses of As_2O_3 for 6 h [$n = 12$ SSc patients (SP)]. For (B) to (G), purified SSc pDCs were cultured with indicated doses of As_2O_3 before tests. (B) Percent of viable SSc pDCs after 24 h ($n = 5$ SP). (C) Percent of BAX^+ cells, and MFI of BAX expression in all pDCs, after 6 h ($n = 3$ SP). (D) MFI of BCL-2 in all pDCs after 6 h ($n = 3$ SP). (E) BAX/BCL-2 MFI ratio after 6 h ($n = 3$ SP). (F) RFI ratios and (G) Percent of positive cells for indicated surface molecules, after 24 h ($n = 5$ SP). Data are represented as mean ± SEM. $^{*}P < 0.05$, $^{**}P < 0.01$ and $^{***}P < 0.001$ by *t*-test.

ratio in pDCs. Moreover, antioxidant NAC did not reverse As_2O_3-induced pDC apoptosis. Collectively, As_2O_3 induced pDC apoptosis *via* the mitochondrial pathway with increased BAX/BCL-2 ratio, and independent of ROS generation.

We observed that As_2O_3 inhibited pDC secretion of IFN-α, which may consequently impair the pDCs' capacity to promote effector $CD8^+$ and Th1 cell responses, to drive B cell activation and plasma cell generation[28]. Meanwhile, the observed inhibition of TNF-α, IL-6 and CXCL10 could reduce capacity of pDCs to upregulate inflammatory reactions and to attract immune cells to sites of infection or inflammation[21].

A 'cross-regulation' effect between IFN-I and TNF-α was previously described in pDCs where TNF-α blockade decreased pDC maturation and promoted their ability to produce IFN-I, leading to possible novel autoimmune side-effects[29,30]. In our study, As_2O_3 inhibited both IFN-α and TNF-α secretion, as well as maturation of pDCs. These effects were probably due to 'double-target' effects of As_2O_3 on both IRF7 and the NF-κB pathways[4,21]. Moreover, the IRF7 pathway seems to be much more sensitive to As_2O_3, as compared to the NF-κB pathway. We observed that clinical relevant concentrations of As_2O_3, which induced neither pDC death nor apoptosis, potently inhibited IFN-α, while leaving

TNF-α unchanged at 6 h of culture. Meanwhile, IRF7 expression and phosphorylation were potently inhibited[28,31]. Indeed, the IFN-I secretion by pDCs is predominantly (albeit not exclusively) mediated through the myeloid differentiation primary response protein 88 (MYD88)-IRF7 pathway[32]. Especially, for the TLR9 ligands CpG ODNs used to activate pDCs in this study, the IFN-I secretion by pDCs seems to be solely mediated through MYD88-IRF7 signaling[33]. We speculate that the IRF7 protein may contain a special domain, offering itself high affinity for soluble trivalent arsenic[34]. Moreover, in pDCs, MYD88-IRF7 is the downstream signaling of TLR-mediated and other cytosolic receptor-mediated nucleic acid sensing. The diminished phosphorylation of IRF7 indicates a probable effect of As_2O_3 on pDC nucleic sensing[35].

Upon TLR7 or TLR9 mediated activation, pDCs mature and express MHC class I (MHCI) and class II (MHCII) molecules and co-stimulatory markers, which operate together to cross-prime $CD8^+$ T cells and present antigen to $CD4^+$ T cells[21]. Mature pDCs also express co-inhibitory molecules such as PD-L1[36,37], and induce regulatory T cell responses[28]. In this study, As_2O_3 inhibited expression of co-stimulatory molecules and chemokine receptors, indicating that it impaired pDCs' trafficking and antigen-presenting capacity.

In line with these observations, we showed that As_2O_3 treatment significantly impaired activated pDCs to promote $CD4^+$ T cell proliferation and Th1/Th22 polarizations. The preferential inhibition of type-I IFN secreted by pDCs after As_2O_3 treatment probably contributed to the deficiency of Th1 pro-inflammatory response[38]. Since abnormal T cell proliferation plays an important role in the pathogenesis of SSc[2,10], and both Th1 and Th22 immune responses are involved in the development of SSc[39,40], these observations highlight an important role of As_2O_3 in modulating T cell responses in SSc. Nevertheless, pDCs regulate B cell growth and differentiation *via* both cytokine secretion and cell-to-cell contact[16−18]. Altered B cell homeostasis characterized by hyperactivity of plasmablasts and autoantibodies production are reported in patients with SSc[41]. We observed in this study that As_2O_3 potently impaired the pDC ability to induce B cell differentiation towards plasmablasts, revealing another important role of As_2O_3 in B cell regulation in SSc.

Regarding effects of As_2O_3 on other immune subsets, previous studies have shown that T and B cells' viability were not significantly affected by clinical relevant concentrations of As_2O_3[42,43]. In addition, As_2O_3 have been reported not to alter viability, but to repress the monocyte-derived dendritic cells' capacity to induce Th1 and Th17 responses[23]. Therefore, both conventional DCs and pDCs probably contribute to As_2O_3 induced immunomodulation *in vivo*. Moreover, it was reported that pDC functions were influenced by a microenvironment enriched in apoptotic cells, leading to Treg increase[44]. Therefore, since clinical relevant concentrations of As_2O_3 induce significant apoptosis of monocytes[45], these apoptotic cells may facilitate As_2O_3-induced pDC immunomodulation *in vivo*.

Chronically activated pDCs are responsible for most of the IFN-α secretion in SSc patients, and play a critical role during the process of fibrosis[7,46]. We observed that similar to healthy pDCs, As_2O_3 induced preferential inhibition of IFN-α secretion, pro-apoptotic effects, and regulatory phenotype in SSc pDCs, indicating that As_2O_3 effects on pDCs from SSc patients were uncompromised.

5. Conclusions

Overall, we have described the pharmacological effects and mechanisms of As_2O_3 on pDCs, which offer an important theoretical explanation for the efficacy of As_2O_3 on SSc, and may pave the way to As_2O_3 utilization in more autoimmune diseases with type-I IFN signature.

Acknowledgments

The authors acknowledge the Association for Training, Education and Research in Hematology, Immunology and Transplantation for the generous and continuous support to the research work. Yishan Ye thanks to China Scholarship Council for financial support (CSC No. 201606320257, China). Mohamad Mohty thanks Prof. J.V. Melo for critical reading of the manuscript.

Author contributions

Yishan Ye: conceptualization, investigation, data curation, writing-original draft. Laure Ricard: investigation, resources, data curation. Lama Siblany: investigation, data curation. Nicolas Stocker: investigation, resources. Frédéric De Vassoigne: investigation. Baptiste Lamarthée: investigation. Arsène Mekinian: resources, writing-review & editing. Mohamad Mohty: conceptualization, writing-review & editing, supervision, funding acquisition. Béatrice Gaugler: conceptualization, writing-review & editing, supervision. Florent Malard: conceptualization, validation, writing-review & editing, supervision, project administration.

Conflicts of interest

The authors declare no conflicts of interest.

Appendix A. Supporting information

Supporting data to this article can be found online at https://doi.org/10.1016/j.apsb.2020.01.016.

References

1. Lo-Coco F, Avvisati G, Vignetti M, Thiede C, Orlando SM, Iacobelli S, et al. Retinoic acid and arsenic trioxide for acute promyelocytic leukemia. *N Engl J Med* 2013;**369**:111−21.
2. Bobe P, Bonardelle D, Benihoud K, Opolon P, Chelbi-Alix MK. Arsenic trioxide: a promising novel therapeutic agent for lymphoproliferative and autoimmune syndromes in MRL/*lpr* mice. *Blood* 2006;**108**:3967−75.
3. Kavian N, Marut W, Servettaz A, Nicco C, Chereau C, Lemarechal H, et al. Reactive oxygen species-mediated killing of activated fibroblasts by arsenic trioxide ameliorates fibrosis in a murine model of systemic sclerosis. *Arthritis Rheum* 2012;**64**:3430−40.
4. Emadi A, Gore SD. Arsenic trioxide—an old drug rediscovered. *Blood Rev* 2010;**24**:191−9.
5. Yu HS, Chen GS, Liao WT, Chang KL, Yu CL. Arsenic induces tumor necrosis factor α release and tumor necrosis factor receptor 1 signaling in T helper cell apoptosis. *J Invest Dermatol* 2002;**119**:812−9.
6. Laurent P, Sisirak V, Lazaro E, Richez C, Duffau P, Blanco P, et al. Innate immunity in systemic sclerosis fibrosis: recent advances. *Front Immunol* 2018;**9**:1702.

7. Ah Kioon MD, Tripodo C, Fernandez D, Kirou KA, Spiera RF, Crow MK, et al. Plasmacytoid dendritic cells promote systemic sclerosis with a key role for TLR8. *Sci Transl Med* 2018;**10**: eaam8458.
8. Kafaja S, Valera I, Divekar AA, Saggar R, Abtin F, Furst DE, et al. pDCs in lung and skin fibrosis in a bleomycin-induced model and patients with systemic sclerosis. *JCI Insight* 2018;**3**:e98380.
9. van Bon L, Affandi AJ, Broen J, Christmann RB, Marijnissen RJ, Stawski L, et al. Proteome-wide analysis and CXCL4 as a biomarker in systemic sclerosis. *N Engl J Med* 2014;**370**:433−43.
10. Liu M, Wu W, Sun X, Yang J, Xu J, Fu W, et al. New insights into $CD4^+$ T cell abnormalities in systemic sclerosis. *Cytokine Growth Factor Rev* 2016;**28**:31−6.
11. de Bourcy CF, Dekker CL, Davis MM, Nicolls MR, Quake SR. Dynamics of the human antibody repertoire after B cell depletion in systemic sclerosis. *Sci Immunol* 2017;**2**:eaan8289.
12. Ricard L, Jachiet V, Malard F, Ye Y, Stocker N, Riviere S, et al. Circulating follicular helper T cells are increased in systemic sclerosis and promote plasmablast differentiation through the IL-21 pathway which can be inhibited by ruxolitinib. *Ann Rheum Dis* 2019;**78**:539−50.
13. Cella M, Facchetti F, Lanzavecchia A, Colonna M. Plasmacytoid dendritic cells activated by influenza virus and CD40L drive a potent TH1 polarization. *Nat Immunol* 2000;**1**:305−10.
14. Ito T, Yang M, Wang YH, Lande R, Gregorio J, Perng OA, et al. Plasmacytoid dendritic cells prime IL-10-producing T regulatory cells by inducible costimulator ligand. *J Exp Med* 2007;**204**:105−15.
15. Rissoan MC, Soumelis V, Kadowaki N, Grouard G, Briere F, de Waal Malefyt R, et al. Reciprocal control of T helper cell and dendritic cell differentiation. *Science* 1999;**283**:1183−6.
16. Jego G, Palucka AK, Blanck JP, Chalouni C, Pascual V, Banchereau J. Plasmacytoid dendritic cells induce plasma cell differentiation through type I interferon and interleukin 6. *Immunity* 2003;**19**:225−34.
17. Ding C, Cai Y, Marroquin J, Ildstad S, Yan J. Plasmacytoid dendritic cells regulate autoreactive B cell activation *via* soluble factors and in a cell-to-cell contact manner. *J Immunol* 2009;**183**:7140−9.
18. Shaw J, Wang YH, Ito T, Arima K, Liu YJ. Plasmacytoid dendritic cells regulate B-cell growth and differentiation *via* CD70. *Blood* 2010; **115**:3051−7.
19. Shen ZX, Chen GQ, Ni JH, Li XS, Xiong SM, Qiu QY, et al. Use of arsenic trioxide (As_2O_3) in the treatment of acute promyelocytic leukemia (APL) II. Clinical efficacy and pharmacokinetics in relapsed patients. *Blood* 1997;**89**:3354−60.
20. Raisova M, Hossini A, Eberle J, Riebeling C, Wieder T, Sturm I, et al. The Bax/Bcl-2 ratio determines the susceptibility of human melanoma cells to CD95/Fas-mediated apoptosis. *J Invest Dermatol* 2001;**117**: 333−40.
21. Swiecki M, Colonna M. The multifaceted biology of plasmacytoid dendritic cells. *Nat Rev Immunol* 2015;**15**:471−85.
22. Honda K, Taniguchi T. IRFs: master regulators of signalling by Toll-like receptors and cytosolic pattern-recognition receptors. *Nat Rev Immunol* 2006;**6**:644−58.
23. Macoch M, Morzadec C, Fardel O, Vernhet L. Inorganic arsenic impairs differentiation and functions of human dendritic cells. *Toxicol Appl Pharmacol* 2013;**266**:204−13.
24. Menon M, Blair PA, Isenberg DA, Mauri C. A regulatory feedback between plasmacytoid dendritic cells and regulatory B cells is aberrant in systemic lupus erythematosus. *Immunity* 2016;**44**:683−97.
25. Lee EF, Fairlie WD, Ottina E, Tarlinton DM, Strasser A, Vikstrom IB, et al. Prosurvival Bcl-2 family members reveal a distinct apoptotic identity between conventional and plasmacytoid dendritic cells. *Proc Natl Acad Sci U S A* 2015;**112**:4044−9.
26. Zhan Y, Chow KV, Soo P, Xu Z, Brady JL, Lawlor KE, et al. Plasmacytoid dendritic cells are short-lived: reappraising the influence of migration, genetic factors and activation on estimation of lifespan. *Sci Rep* 2016;**6**:25060.
27. Kale J, Osterlund EJ, Andrews DW. BCL-2 family proteins: changing partners in the dance towards death. *Cell Death Differ* 2018;**25**:65−80.
28. Reizis B. Plasmacytoid dendritic cells: development, regulation, and function. *Immunity* 2019;**50**:37−50.
29. Cantaert T, Baeten D, Tak PP, van Baarsen LGM. Type I IFN and TNFα cross-regulation in immune-mediated inflammatory disease: basic concepts and clinical relevance. *Arthritis Res Ther* 2010;**12**:219.
30. Conrad C, Di Domizio J, Mylonas A, Belkhodja C, Demaria O, Navarini AA, et al. TNF blockade induces a dysregulated type I interferon response without autoimmunity in paradoxical psoriasis. *Nat Commun* 2018;**9**:25.
31. Kim S, Kaiser V, Beier E, Bechheim M, Guenthner-Biller M, Ablasser A, et al. Self-priming determines high type I IFN production by plasmacytoid dendritic cells. *Eur J Immunol* 2014;**44**:807−18.
32. Honda K, Yanai H, Negishi H, Asagiri M, Sato M, Mizutani T, et al. IRF-7 is the master regulator of type-I interferon-dependent immune responses. *Nature* 2005;**434**:772−7.
33. Honda K, Ohba Y, Yanai H, Negishi H, Mizutani T, Takaoka A, et al. Spatiotemporal regulation of MyD88−IRF-7 signalling for robust type-I interferon induction. *Nature* 2005;**434**:1035−40.
34. Shen S, Li XF, Cullen WR, Weinfeld M, Le XC. Arsenic binding to proteins. *Chem Rev* 2013;**113**:7769−92.
35. Kim T, Pazhoor S, Bao M, Zhang Z, Hanabuchi S, Facchinetti V, et al. Aspartate-glutamate-alanine-histidine box motif (DEAH)/RNA helicase A helicases sense microbial DNA in human plasmacytoid dendritic cells. *Proc Natl Acad Sci U S A* 2010;**107**:15181−6.
36. Diana J, Brezar V, Beaudoin L, Dalod M, Mellor A, Tafuri A, et al. Viral infection prevents diabetes by inducing regulatory T cells through NKT cell-plasmacytoid dendritic cell interplay. *J Exp Med* 2011;**208**:729−45.
37. Wolfle SJ, Strebovsky J, Bartz H, Sahr A, Arnold C, Kaiser C, et al. PD-L1 expression on tolerogenic APCs is controlled by STAT-3. *Eur J Immunol* 2011;**41**:413−24.
38. Swain SL, McKinstry KK, Strutt TM. Expanding roles for $CD4^+$ T cells in immunity to viruses. *Nat Rev Immunol* 2012;**12**:136−48.
39. Antonelli A, Ferri C, Fallahi P, Colaci M, Giuggioli D, Ferrari SM, et al. Th1 and Th2 chemokine serum levels in systemic sclerosis in the presence or absence of autoimmune thyroiditis. *J Rheumatol* 2008;**35**: 1809−11.
40. Fard NA, Azizi G, Mirshafiey A. The potential role of T helper cell 22 and IL-22 in immunopathogenesis of multiple sclerosis. *Innovat Clin Neurosci* 2016;**13**:30−6.
41. Sato S, Fujimoto M, Hasegawa M, Takehara K. Altered blood B lymphocyte homeostasis in systemic sclerosis: expanded naive B cells and diminished but activated memory B cells. *Arthritis Rheum* 2004; **50**:1918−27.
42. Gupta S, Yel L, Kim D, Kim C, Chiplunkar S, Gollapudi S. Arsenic trioxide induces apoptosis in peripheral blood T lymphocyte subsets by inducing oxidative stress: a role of Bcl-2. *Mol Canc Therapeut* 2003;**2**:711−9.
43. Baysan A, Yel L, Gollapudi S, Su H, Gupta S. Arsenic trioxide induces apoptosis *via* the mitochondrial pathway by upregulating the expression of Bax and Bim in human B cells. *Int J Oncol* 2007;**30**:313−8.
44. Bonnefoy F, Perruche S, Couturier M, Sedrati A, Sun Y, Tiberghien P, et al. Plasmacytoid dendritic cells play a major role in apoptotic leukocyte-induced immune modulation. *J Immunol* 2011;**186**:5696−705.
45. Lemarie A, Morzadec C, Merino D, Micheau O, Fardel O, Vernhet L. Arsenic trioxide induces apoptosis of human monocytes during macrophagic differentiation through nuclear factor-kappaB-related survival pathway down-regulation. *J Pharmacol Exp Therapeut* 2006;**316**:304−14.
46. Kim D, Peck A, Santer D, Patole P, Schwartz SM, Molitor JA, et al. Induction of interferon-alpha by scleroderma sera containing autoantibodies to topoisomerase I: association of higher interferon-alpha activity with lung fibrosis. *Arthritis Rheum* 2008;**58**:2163−73.